J. Appl. Comput. Mech., 11(1) (2025) 264-273
DOI: 10.22055/jacm.2024.46304.4496

ISSN: 2383-4536
jacm.scu.ac.ir

Shahid Chamran University of Ahvaz

Journal of Applied and Computational Mechanics

Research Paper

Complexity-Aware Design Analysis of the Efficiency in Darrieus Vertical Axis Wind Turbines

Rodrigo S. Vieira[1], Ana Pavlovic[2], Cristiano Fragassa[2], Elizaldo D. dos Santos[3], Adriane P. Petry[1]

[1] Department of Mechanical Engineering, Federal University of Rio Grande do Sul (UFRGS), Sarmento Leite St., 425, Porto Alegre 90040-001, Brazil, Email: spotorno.furg@gmail.com (R.S.V.); adrianep@mecanica.ufrgs.br (A.P.P.)

[2] Department of Industrial Engineering, University of Bologna, Viale Risorgimento 2, 40136 Bologna, Italy, Email: ana.pavlovic@unibo.it (A.P.); cristiano.fragassa@unibo.it (C.F.)

[3] School of Engineering Universidade Federal do Rio Grande, Italia Av., km 8, 96203-900, Rio Grande-RS, Brazil, Email: elizaldosantos@furg.br

Received March 07 2024; Revised June 25 2024; Accepted for publication July 10 2024.
Corresponding author: A. Pavlovic (ana.pavlovic@unibo.it)

Abstract. This study proposes a numerical investigation for assessing the primary design parameters influencing the efficiency of a Darrieus type vertical axis wind turbine. The methodology consists in the numerical solution of the continuity and momentum equations utilizing the Unsteady Reynolds Averaged Navier-Stokes (URANS) approach. The turbulence closure model is the SST $k-\omega$, and the Finite Volume Method is applied to solve the three-dimensional geometries. The findings confirm that variations in solidity and aspect ratio of twisted blade turbines, in comparison to straight blade configurations, exert a similar influence on the torque coefficient, surpassing the impact of blade torsion angle variations. Results corroborated previous findings of literature about the fluctuations in the torque coefficient (C_m) being smoothed in 55% when helical blades are used in comparison with straight configuration. However, the increase in blade torsion angle corresponded to a decrease in the torque coefficient, with maximum difference of 37% when solidity (σ) is $\sigma = 0.75$ and the ratio between height and radius of the turbine is $H/R = 1.5$. Results also demonstrated that the increase in the solidity from $\sigma = 0.4$ to 0.8 reduced the effect of the ratio H/R on the C_m. The increase of σ allowed a gain in C_m of nearly 60%. For constant σ and tip speed ratio (λ), the increase of H/R from 2.5 to 7.5 led to an increase of 79% in C_m. In general, results supplied a guideline on the influence of λ, twisted angle, σ, and H/R on the performance of helical Darrieus turbines.

Keywords: Vertical axis wind turbine; Twisted blade Darrieus; Design; Aerodynamics; Numerical simulation; Finite volume method.

1. Introduction

Wind energy, supplying about 8% of global electricity from 900 GW capacity, is a key renewable source in many countries, e.g., Denmark (45%) and the UK (25%) [1]. It also serves as the primary renewable energy in other countries like US, where onshore wind is among the most cost-effective electricity generation methods [2]. Moreover, according to McKenna et al. [3] the most significant non-hydropower renewable energy is the onshore wind energy which has increased from 13% to 24% of renewable energy matrix in the period from 2009 to 2018. Other important aspect is the reduction of costs related with offshore and onshore wind energy, that has decreased 60% and 32%, respectively, since 2015 [4].

Horizontal axis wind turbines (HAWTs), making up 99% of the market, are preferred for large-scale installations due to their high energy efficiency [5]. In contrast, vertical axis wind turbines (VAWTs) are better suited for domestic and urban areas because of their versatility in confined spaces and directional wind capture, despite producing less energy. VAWTs offer benefits like lower noise and easier maintenance, highlighting the need for improved performance for broader adoption [6].

The present analysis explores how blade design influences efficiency in the case of Darrieus type VAWTs, focusing on how the twist angle of blades affects energy capture from various wind speeds and directions, and how generated torque impacts energy conversion efficiency [7]. And they are valued for their high efficiency within VAWTs, achievable by selecting optimal aerodynamic blade profiles [7].

Straight-blade Darrieus VAWTs, known for their simplicity with three vertical blades set at $120°$, offer output torque that can be easily modulated by changes in the design parameters [8]. This is also the case of an H-rotor, where the blades are positioned in a semilunar shape around the central shaft [9]. The twisted-blade Darrieus turbine, designed for reducing the torque fluctuation and improvement of self-starting capabilities, features a helical shape that performs well at high angular velocities even in low flow,

Published online: July 22 2024

minimizing torque fluctuations [10, 11]. These are only a very few cases that highlight the general concept of the importance of combining shapes and fluid dynamics in the optimization of turbines.

In [12], for instance, Darrieus turbines with three and four blades, and a NACA0018 profile, showed that increased twist angles reduce power output by lowering lift force and torque. Other analyses, as in [13-28], investigated the effect of specific geometric parameters (chord length, twist angle, pitch angle, rotor diameter and rotor height) on performance of Darrieus turbines (especially turbine torque and power).

Another key factor is the solidity, equal to the ratio of the total rotor area (the area covered by the blades) to the swept area of the rotor (the total area through which the blades move) [13]. The solidity is influenced by the main turbine geometric parameters as rotor radius, number of blades and chord length [28]. When high σ is used, that is, a large chord length and a small diameter, there is an increase in the turbine power coefficient for a low tip speed ratio (λ) value, and the torque production is enhanced using a high chord length [29]. However, when analyzing high λ values, a lower σ leads to a higher power value [14]. Furthermore, the blade twist angle emerged as a crucial parameter significantly enhancing turbine efficiency, without being affected by λ [17,18].

Research was also focused on enhancing Darrieus turbines by exploring new strategies such as angle of attack variation devices, novel shapes, and geometric adjustments to boost performance, emphasizing the critical role of geometric parameters. For instance, in [18], the effect of geometry on the power coefficient was investigated in the case of tidal turbines. Despite of tidal and wind turbines differences, the relationship between blade shapes, fluid dynamics, structural design, efficiency and usability have some similarities. Therefore, strategies for design of one kind of turbine can be tested to improve the performance of the other one. Tjiu et al. [19] performed a very interesting review about the main configurations of Darrieus vertical axis wind turbine, showing a timeline of the development of several rotors and drawbacks that prevented the development of some rotors in large scale. In [20], e.g., a way to increase the maximum power coefficient varying the angle of attack as the turbine rotates, up to 0.35 of the power coefficients was discussed. In [21], where a Savonius turbine combined with a Darrieus one was considered, it was demonstrated that the radius of this hybrid turbine had a greater influence than the twist angle, in the same way the radius that led to the best power coefficient is close to the radius of the Darrieus turbine. In [25], e.g., a two-dimensional study was carried out to detect the aerodynamic forces in the case of a Darrieus turbine during its start-up. In [26] Darrieus turbines were considered respect to the effect of offshore wind turbulence, confirming the importance of aerodynamics in the optimal design (e.g., structural dimension, lifespan). In [27] a direct comparison was conducted between 2D and 3D approaches for H-Darrieus turbines and stall phenomena confirming the benefits of a 3D analysis for accurately assessing optimal design parameters, despite computational challenges. Other strategies such as the use of slotted blades have also been used to reduce the flow separation and improve the turbine performance [30]. Several recommendations have been achieved with the use of the computational fluid dynamics (CFD), that has evolved significantly over time, both in computational terms and in turbulence models [31]. Recently, Tominaga et al. [32] performed an important review about research progresses and challenges on the use of computational fluid dynamics (CFD) for complex urban aerodynamics and microclimates. Moreover, important progresses have been made in the use of computational intelligence algorithms to obtain recommendations about the best operational parameters of wind turbines. For instance, Kasmaiee et al. [33, 34] associated the use of CFD, neural networks and genetic algorithms to determine the parameters of blowing jet that maximizes the lift coefficient in an airfoil applied in wind turbine.

Despite CFD's widespread use, research on Darrieus turbines with twisted blades in turbulent airflow is limited, especially with air as the working fluid. While geometric factors for twisted turbines are assumed to be like those for straight-bladed turbines or those used in tidal energy conversion, specific investigations are required to confirm this. Despite many studies, a comprehensive understanding of how design parameters interact, and optimal configurations are achieved remains elusive. This knowledge gap hampers both existing turbine optimization and the development of crucial advanced models for wind engineering [31].

2. Materials and Methods

The present study is based on [14], maintaining the same σ, aspect ratio and aerodynamic profile, but using a different turbulence model and a twist angle in the blade profile. In the work of [14], it was directly compared the effects of blade torsion in relation to a straight-blade vertical axis turbine, thus analyzing these effects not only on turbine torque and power, but also on the flow behavior. More precisely, it was obtained theoretical recommendations about the influence of the twist angle over the device torque coefficient and showing the pressure field and eddy viscosity around the blade's profiles. Results demonstrated that for low tip speed ratios, larger chord values and smaller turbine diameters led to an increase in power. However, for a high value of the tip speed ratio, the opposite was advantageous, considering the same conditions for the turbine.

For the simulation of incompressible and turbulent flows in the three-dimensional domain of the twist Darrieus turbine, the unsteady time-averaged conservation equation of mass and the balance of momentum equations are numerically solved by means of a code based on the Finite Volume Method. The standard $k-\omega$ SST model is used here for closure of time-averaged equations. It is also used an interface region between the mobile mesh (rotational domain) and the fixed mesh. This condition prevents distortions in the rotational movement imposed on the mesh, since the mobile region of the rotor rotates with a certain angular velocity.

Similarly, the computational domain follows the same ratios between height of the domain and diameter of the rotor and length of the domain and diameter of the rotor presented in [14]. More precisely, it is considered a radius of $5D$ for the region in front of the rotor and a length of $7D$ for the region after the rotor, where D is the turbine diameter. The depth (in the normal plane of Fig. 1) is given by the height of the turbine. These dimensions were established according to the study, i.e., depending on the adopted value of σ the diameter is influenced and the dimensions of the domain change. Fig. 1(a) represents the domain simulated here and the boundary conditions used in it, while Fig. 1(b) illustrates the detail of turbine with twist angle. The main parameter of study is the torque coefficient. The turbine dimensions follow the specifications of [14], where it has a height of $H = 0.6$ m and a diameter of $D = 0.74$ m, a blade chord of $c = 0.2$ m with a NACA0015 profile. The wind speed imposed at the entrance to the domain is $U_\infty = 12$ m/s.

The input velocity boundary condition is used at the curved input of the domain, applying an input prescribed velocity only on the x-axis of the domain. In the blade, the boundary condition imposed is a non-slip and impermeable wall (velocities in three spatial coordinates are set to zero). At the exit of the domain, there is a pressure outlet condition, which is equal to the atmospheric pressure or null gauge pressure. The side, top and bottom walls are considered with the boundary condition of symmetry ($\partial u_i/\partial x_2 = 0$, where $i = 1$,2 and 3 and represents the spatial coordinate axis x, y and z, respectively).

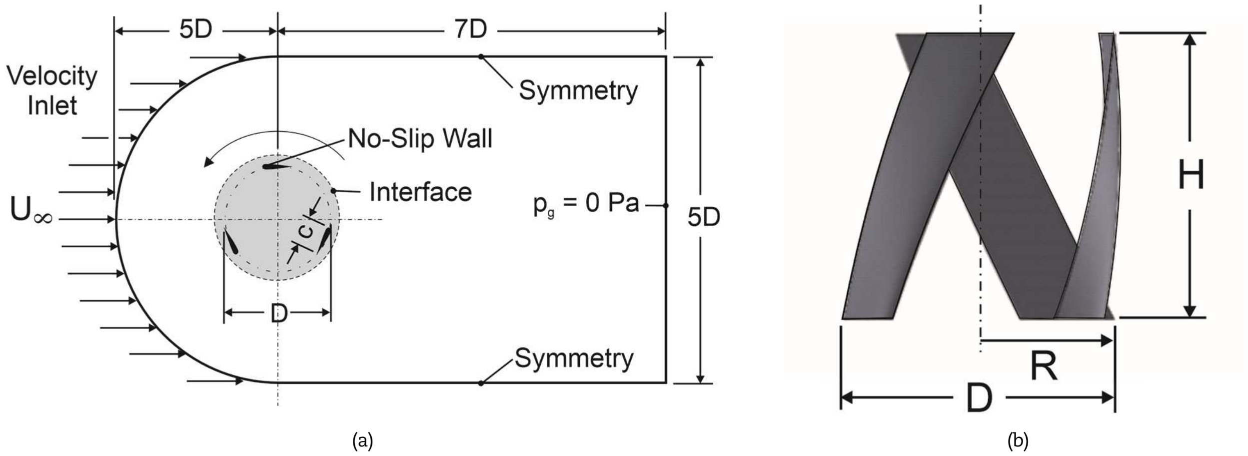

Fig. 1. Computational domain of the Darrieus turbine investigated: (a) imposed boundary conditions; (b) dimensions of turbine with twist angle.

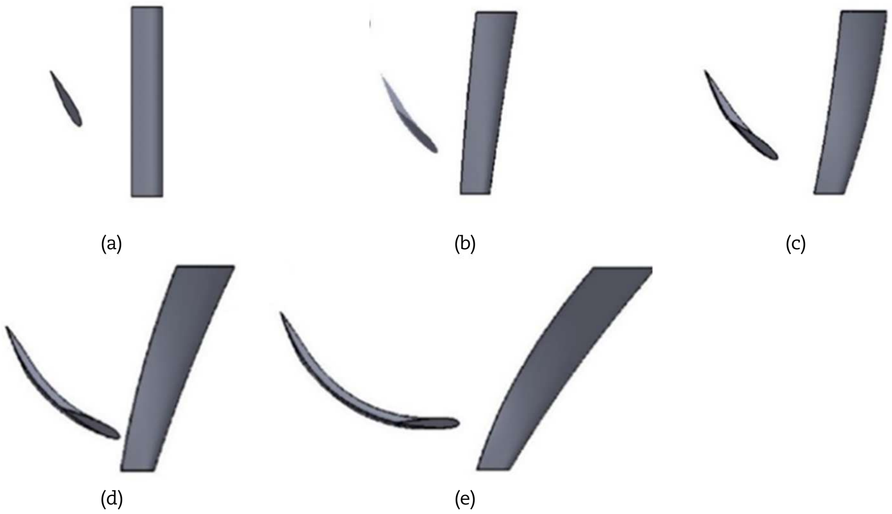

Fig. 2. Superior and front views respect to different twist angles of the turbine blades: (a) straight turbine ($0°$), (b) angle = $15°$, (c) angle = $22.5°$, (d) angle = $35°$, and (e) angle = $60°$.

The main analysis is related to the torsion angle of the blade. In [14], it was investigated a straight blade. Here, it is carried out a variation of torsion angle of the blade by increasing the angle in relation to the straight blade from $15°$ to $60°$. The effect of the twist angle over the torque coefficient generated in the central axis of the turbine is investigated, considering a tip speed ratio equal to 1.2, so that the angular velocity is 24 rad/s. It is worth mentioning that the main purpose in this investigation is to analyze the tendency about the effect of the angle on the performance parameter C_m, and investigate the influence of other parameters as H/R, σ, and λ on the turbine performance. This associated with the complexity to simulate each case in terms of geometry and mesh generation, as well as, computational effort, restricted the number of cases studied. The angles were selected in such a way to have a homogeneous distribution on the search space, with a slight refinement in its intermediate region.

Figure 2 shows the difference between a straight blade Darrieus turbine and twisted blade Darrieus turbine with the twist angle of $15°$, $22.5°$, $35°$ and $60°$. The increase of the angle generates a large variation in the geometry, increasing the turbine contact area. As can be seen, the blade starts with the same angle and in the same position, however, as the twist angle increases it ends in a different position, with a great variation in relation to the initial position.

Figure 3 shows the difference between the turbine with straight blades and the turbine with twisted blades, for the case with $60°$. Even though both have the same diameter and height, there is a difference between the areas of the blades due to their torsion. This effect, as previously mentioned, causes greater contact between the blades and the flow.

After verifying the model using the straight-blade turbine referred to [14], with the same constructive and flow characteristics, a comparative study is performed here between the torque coefficient obtained with straight blades turbine [14] and a $45°$ twisted blades turbine, with the same characteristics already presented, for different λ. Table 1 shows the different twist angle used in this study.

Table 1. Studied cases with different twist angles.

Case	Twist angle
1	0° *
2	15°
3	22.5°
4	35°
5	45°
6	60°

* Straight blade.

(a) (b)

Fig. 3. Difference between the turbine with straight blades and the turbine with twisted blades ($60°$).

The analysis is also carried out by varying the aspect ratio of the turbine. Initially, a height of $H = 0.6$ m is used, as in [14], followed by the additional configurations of $H = 0.8$ and 1.0 m, thus varying the aspect ratio according to Table 2, valid in the case of a turbine with $45°$ twisted blades.

The solidity (σ) and tip speed ratio (λ) are given, respectively, by:

$$\sigma = \frac{Nc}{D} \tag{1}$$

$$\lambda = \frac{\Omega R}{U_\infty} \tag{2}$$

where N is the number of blades, c is the blade chord, D the diameter of the rotor, Ω is the angular velocity of the rotor, R is the radius of the rotor and U_∞ is the free stream velocity upstream the turbine.

This study shows the results for the torque coefficient in different cases, for different aspect ratios (H/R) and σ, showing the effect of these parameters for a twisted-blade turbine.

2.1. Mathematical and numerical modeling

The URANS (Unsteady Reynolds-Averaged Navier-Stokes) methodology is used to solve the transient and turbulent flows. It is considered here incompressible, turbulent flows, without body forces in a three-dimensional domain [35–39]. Time-averaged conservation of mass and balance of momentum equations are solved by means of Finite Volume Method (FVM), more precisely with the FLUENT software [40–42]. For modeling of this problem, the continuity equation is given by [43]:

$$\frac{\partial \overline{u_i}}{\partial x_i} = 0 \tag{3}$$

where u_i and x_i are the velocity in i-direction and spatial coordinate (i = 1, 2 and 3, which represents the directions x, y and z, respectively). The time-averaged equation of the momentum is written by [43]:

$$\rho\frac{\partial \overline{u_i}}{\partial t} + \rho\overline{u_j}\frac{\partial \overline{u_i}}{\partial x_j} = -\frac{\partial \bar{P}}{\partial x_i} + \frac{\partial}{\partial x_j}\left(\mu\left(\frac{\partial \overline{u_i}}{\partial x_j} + \frac{\partial \overline{u_j}}{\partial x_i}\right) - \overline{\rho u_i' u_j'}\right) \tag{4}$$

where ρ is the fluid density, μ is the dynamic viscosity, t is the time, P denotes the pressure, and the Reynolds stresses are represented by $\overline{\rho u_i' u_j'}$. The Reynolds stresses can be related with the time-averaged deformation rate by the Boussinesq approximation [35]. Then, the momentum equation can be rewritten by [35, 43]:

$$\rho\frac{\partial \overline{u_i}}{\partial t} + \rho\overline{u_j}\frac{\partial \overline{u_i}}{\partial x_j} = -\frac{\partial \bar{P}}{\partial x_i} + \frac{\partial}{\partial x_j}\left((\mu + \mu_t)\left(\frac{\partial \overline{u_i}}{\partial x_j} + \frac{\partial \overline{u_j}}{\partial x_i}\right)\right) \tag{5}$$

The turbulent viscosity (μ_t) is represented by [35]:

$$\mu_t = min\left(\frac{\rho k}{\omega}; \frac{\mathrm{a}_1 \rho k}{\mathrm{S}F_2}\right) \tag{6}$$

where k is the turbulent kinetic energy, ω is the specific dissipation rate, S is the invariant measure of the strain rate, F_2 is a blending function used to modulate the closure model to be used depending on the region of the flow. Standard coefficients available in FLUENT software were used in the simulations: $\mathrm{a}_1 = 0.31$, $\beta = 0.09$, $\alpha_1 = 5/9$, $\beta_1 = 3/40$, $\sigma_k = 0.85$, $\sigma_\omega = 0.5$, $\sigma_2 = 0.44$, $\beta_2 = 0.0828$, $\sigma_2 = 1$, and $\sigma_{\omega 2} = 0.856$.

Table 2. Aspect ratio in relation to three different solidity values ($\sigma = 0.4$, 0.6, and 0.8).

σ	H/R	H [m]	$R = D/2$ [m]	λ
0.4	0.81	0.6	0.74	1.6
0.4	1.08	0.8	0.74	1.6
0.6	1.20	0.6	0.50	1.2
0.4	1.35	1.0	0.74	1.6
0.6	1.60	0.8	0.50	1.2
0.8	1.62	0.6	0.37	1.0
0.6	2.00	1.0	0.50	1.2
0.8	2.16	0.8	0.37	1.0
0.8	2.70	1.0	0.37	1.0

The turbulence model chosen to solve the problem is a two-equation model derived from the original $k-\omega$ formulation presented by [38] and named $k-\omega$ SST (Shear Stress Transport), which is implemented in the software FLUENT, version 21 [39]. In this closure modeling two main changes were made in comparison with the original formulation of $k-\omega$ model. The first was the reformulation of the model with the addition of a combination function that kept the $k-\omega$ modeling in the region close to the wall, changing to the $k-\varepsilon$ formulation as the flow is modeled in regions of boundary layer far from the walls. The second change is the modification of the definition of turbulent viscosity to include the transport of turbulent shear stress (SST) as seen in [35, 36, 38]. To avoid the flaws found in the $k-\varepsilon$ and $k-\omega$ turbulence models, this model is selected demonstrating the same advantages acquired in other models. For instance, models based on ε cannot adequately predict the behavior of the turbulent boundary layer until the separation, while its application is recommended in free shear flows, based on the recommendations described in the literature [12]. It is worth noting that, the URANS closure model requires a computational effort significantly lower than other approaches as large eddy simulation (LES) and direct numerical simulation (DNS), which guided the choice for the use of URANS modeling. Among the closure models into URANS framework, the $k-\omega$ SST has shown the most appropriate for simulation of free-shear basin flows, as those found in turbulent flows over aerodynamic profiles. Moreover, recent works related with simulation in turbulent flows over turbines have employed this closure model [10, 21, 27] justifying its used in the present work. The time-averaged conservation equation of mass and the equation of the balance of momentum, as well as the differential transport equations of the turbulence model $k-\omega$ SST, are solved using the finite volume method (MVF) using FLUENT software [39–41].

The mesh generated in the computational domain for the elaboration of the simulations is created in a three-dimensional domain with a spatial discretization of approximately 3.7 million elements. The mesh refinement has a prismatic refinement in the blade region, with a growth region of 1.2 with a first layer thickness of 10^{-5} m consisting of 24 elements along the profile wall. This layer is necessary to improve the accuracy of the near-wall flow solution. In the region close to the blade, to correctly calculate the boundary layer profile, it is important to refine the mesh in the orthogonal direction of the solid walls. This refinement can be guided by the variable y^+ which is given by [42]:

$$y^+ = \frac{y\sqrt{\frac{\tau_w}{\rho}}}{\nu} = \frac{yu_\tau}{\nu} \tag{7}$$

where τ_w is the shear stress in the wall region, ν is the kinematic viscosity and u_τ is the friction velocity. The dimensionless distance from the wall is a way to see if the parameters used in the mesh are acceptable for different turbulence models, and for the $k-\omega$ SST model this variable is acceptable for values smaller than 1.0 [44]. In the present study the mean magnitude of y^+ was lower than 1.0 in the turbine blades.

A pressure-based solver was select to numerically solve the problem. A coupled algorithm was selected for velocity-coupling. For the treatment of advective terms a second order upwind was selected. The physical problem is time dependent, therefore, an unsteady implicit and iterative solution is applied. It is worth mentioning that, after some period, the flow reaches a steady condition, i.e., the fluctuations of the fields and parameters stabilize as a function of the time. Then, the parameters as the torque coefficient are analyzed when the flow reaches the steady condition.

Concerning the residuals, values of 10^{-5} were used for the continuity, and 10^{-6} for the momentum, and transport equations. For some time-steps the residuals reached to magnitudes of 2×10^{-5} for the continuity equation, being the time advancement performed by the achievement of the maximum number of iterations for each time step. This convergence is considered acceptable due to the complexity of the domain and physical problem. These difficulties have led to the consideration of residuals of 10^{-4} for mass conservation equation in the literature, e.g., Karimian and Abolfazl [10]. The residuals are the differences in values between each iteration performed. All the solutions were simulated considering the transient regime. The time step used was $\Delta t = 0.001$ s, with 60 iterations per step and 1000 time steps, totaling 60000 iterations and a physical simulation time of $t_f = 1.0$ s. The time step used were based on the previous studies of literature, see [10, 16]. For each time step, it is imposed a change of $0.00628°$ in the rotational domain moving the blades of the Darrieus turbine.

For the numerical simulation, a desktop computer with AMD Ryzen 7 3800x CPU of 4.4 GHz and 32 Gb of RAM was used. The actual physical time used to perform each of the simulated cases was around of forty-eight (48) to seventy-two (72) hours of computational simulation.

2.2. Problem verification

For the mesh independence study, the rotor model with a chord of $c = 200$ mm and a $\lambda = 2$ was chosen, the same used in [14]. The turbine data are the same used in the continuation of the study, where it has a radius of $R = 370$ mm and a height of $H = 600$ mm. The torque coefficient is given by:

$$C_m = \frac{T}{\frac{1}{2}\rho ARU_\infty^2} \tag{8}$$

where T is the turbine torque, A is the projected area of the rotor ($A = H.D$).

In [14], it was obtained a torque coefficient of $C_m = 0.285$. For the verification procedure, different meshes were tested and the results obtained for the grid independent configuration are compared with those presented in the literature. Figure 4 shows the mesh domain generated for the model used here. More precisely, Fig. 4(a) shows the whole domain with the strong refinement in the surfaces of Darrieus blades, while Fig. 4(b) shows a detailed view of the refinement in the near wall region of the blade, using several prism layers in the normal direction of the blade surfaces.

Table 3 shows the values found in the mesh sensibility study. In this test, 3 meshes are implemented, where each one represents a discretization where the number of elements of the refined mesh has two times the number of elements of the previous coarse mesh and the physical problem is simulated until $t = 1.0$ s. The last cycles of turbine rotation are used to calculate the mean magnitudes of C_m presented in Table 3. In terms of time interval, the period in the range $0.8\text{ s} \le t \le 1.0\text{ s}$ is used to obtain the time-averaged magnitudes of C_m. Note that the difference between the values found for meshes 2 and 3 is slightly greater than 0.04%, and the difference between mesh 1 (mesh considered coarser) and mesh 2 is around 1.8%.

Therefore, mesh 2 was chosen as a mesh that complies with the requirements of the study, since it has results with few variations and lower computational effort in comparison with mesh 3. It is also noted that the difference in the magnitude of C_m between the chosen mesh (mesh 2) and the reference value, given by [14], is less than 3.8%.

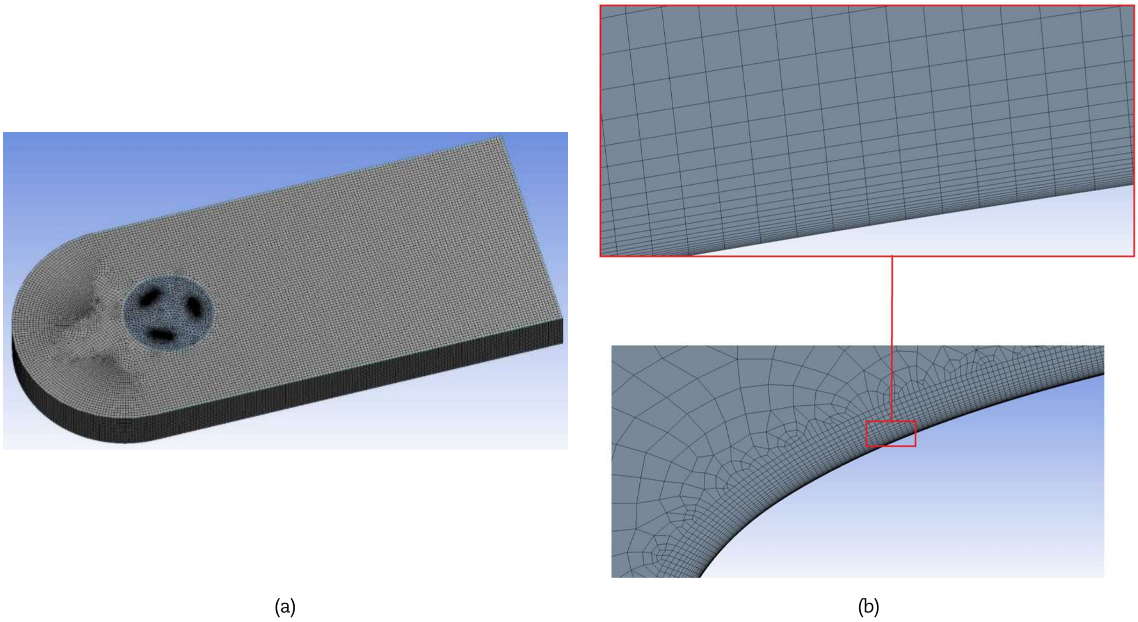

Fig. 4. Computational domain of the model: (a) general view, (b) detailed view in blade region.

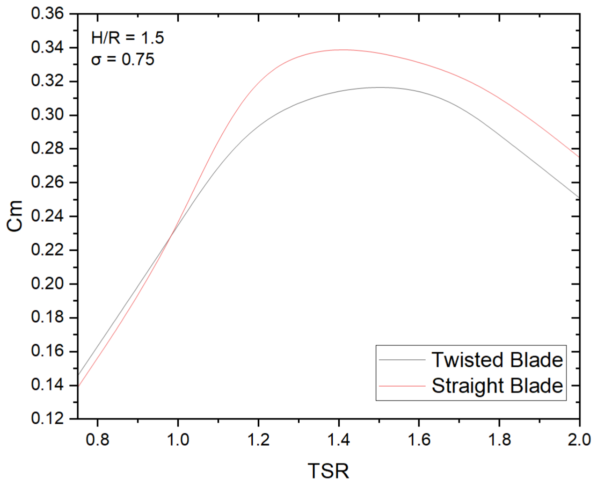

Fig. 5. Influence of λ over the torque coefficient (C_m) for twisted and straight blades Darrieus turbines.

The difference between the values found here and in [14] can be attributed to the difference of methodology for approach of turbulence. In [14], the Large Eddy Simulation (LES) is used for closure of turbulence, while in the present study the URANS methodology is used. Despite that, the behavior found between the two studies is convergent. It is worth mentioning that the LES approach conducts to a much higher computational effort than the URANS closure modeling, which would avoid the achievement of recommendations about the geometrical configuration of the twisted blade over the turbine performance due to the time needed to explore several geometric variations of the twisted blade turbine.

3. Results and Discussion

Figure 5 shows the effect of the λ over the torque coefficient (C_m) for a straight and twisted configuration with a twist angle of $45°$. There is agreement in the behavior observed in both studies (twisted and straight blades). There is a decrease in the average torque generated by the turbine with twisted blades in comparison with straight blades, as expected. The minimum and maximum differences in calculated torque are approximately 3% and 11%. The main differences are noted for $\lambda \geq 1.0$, indicating a higher influence of the shape of blade for higher magnitudes of λ. The maximum power can be achieved for $\lambda = 1.8$, being the straight blade almost 8% higher than twisted blade. It is also noticed that the highest magnitude of C_m is obtained for different λ for the different configurations. The increase in λ for a fixed geometry (same blade radius and height) and the same free wind velocity means an increase in the turbine rotation velocity. So, as λ increases, the turbine rotation increases. Due to the geometric variation of the twisted blades and their influence on turbulent effects, the torque coefficient begins to fall and become smoother.

Table 3. Results of the grid independence study.

	C_m	Difference (%)	Number of Elements
Mesh 1	0.2697	-	1.8×10^6
Mesh 2	0.2746	1.8	4.8×10^6
Mesh 3	0.2747	0.04	8.4×10^6
Lee and Lim [12]	0.2850		

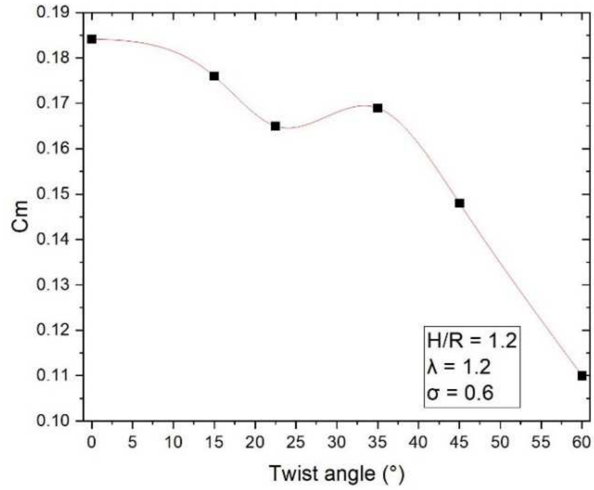

Fig. 6. Influence of the twist angle over the torque coefficient (C_m) for $H/R = 1.2$, $\lambda = 1.2$ and $\sigma = 0.6$.

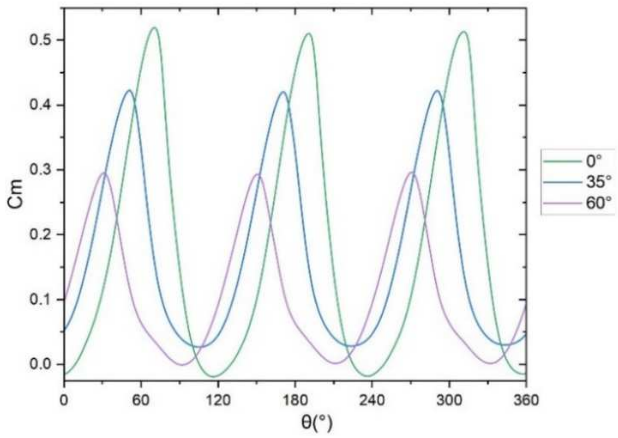

Fig. 7. The torque coefficient (C_m) in one rotation for three different twist angles.

After that, a study related to the angle of twist is performed for $\lambda = 1.2$, the ratio between the turbine height and radius of $H/R = 1.2$, and solidity of $\sigma = 0.6$. As can be seen in Fig. 6, for the present conditions, there is a drop in the torque coefficient as the blade angle becomes larger, with a total reduction of 37% when the angle changes from $15°$ to $60°$. One possible reason for this behavior is related to the flow inside the blades, which generate a drop in the lift force.

Figure 7 shows the difference in torque coefficient for three different twisted angles, representing a complete rotation of the turbine. It is observed that the torque fluctuation decreases with increasing twisted angle. Therefore, there is a reduction in the average torque according to the variation of the twist angle. The twist angle of $0°$ represents a straight blade Darrieus turbine. Results also demonstrate that the peak of torque coefficient happened for different rotation angles of the rotor movement. It is important to mention that the increase of the twisted angle led to a more homogeneous distribution of vortex shedding along the spanwise direction of the blade and a reduction of pressure difference between the back and upper surfaces of the blade. These effects led to a decrease on the magnitude of the torque fluctuation and changes of magnitude of C_m as a function of angle of rotation of the turbine, leading to the patterns observed in Fig. 7 for the different twist angles.

To illustrate the drop of C_m with the increase of twist angle, Fig. 8 illustrates a comparison between the pressure fields in a plane in the half height of the turbine for the twist angles of $15°$ and $60°$, Figs. 8(a) and 8(b), respectively. It is possible to perceive a difference between the pressure fields generated for the two conditions. It is worth mentioning that both turbines are under the same flow conditions, $\lambda = 1.2$, and both have the same dimensions of height and diameter of the turbine, with $H = 0.6$ m and $D = 1$ m, respectively. It is possible to verify that the pressure field for a turbine with a smaller angle, $15°$, is under a greater pressure gradient between the internal and external parts of the turbine blade. This pressure difference collaborates to increase the torque generated by the turbine. In the turbine with a larger angle, $60°$, a lower intensity and less uniform pressure field can be observed along the entire height of the blade. This difference between one turbine and another also highlights the difference in its performance.

Figure 9 demonstrates the variation of turbulent viscosity for a twist angle of $15°$ and $60°$. As the twist angle increases, the intensity of turbulent viscosity also increases. This increase is related to the complexity that the increase in the twist angle gives to the flow inside turbine, leading to perturbations in the flow over turbines that decreases the magnitude of torque coefficients.

As mentioned previously, the aspect ratio is dependent on the height and diameter of the turbine. The aspect ratio study is limited to a range of heights to try to achieve high aspect ratio values, as there is also a dependence on the diameter. Therefore, for high aspect ratio values, another study is carried out. In it, the wind speed is reduced to 6 m/s and a radius of 0.24 m is used, thus obtaining higher aspect ratio values by changing the height of the turbine. Without these changes, the turbine would be very tall, increasing the computational effort involved. This reduction in velocity is also caused by the limitations of the model, since with the imposition of a rotation, once again the turbine starts to behave like a generating flow machine due to its high rotation.

In Fig. 10 it is evident that, for the same σ value, the turbine with a higher aspect ratio provides a higher torque coefficient. However, as there is an increase in σ, the behavior changes, and a lower aspect ratio leads to a greater torque coefficient, as can be seen for the curve representing $\sigma = 0.8$. This reinforces that a higher aspect ratio produces a higher starting torque at low λ.

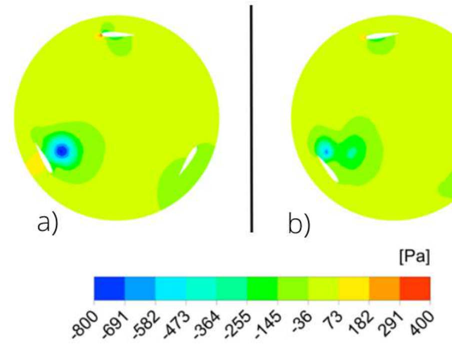

Fig. 8. Pressure fields: (a) twist angle = $15°$; (b) twist angle = $60°$.

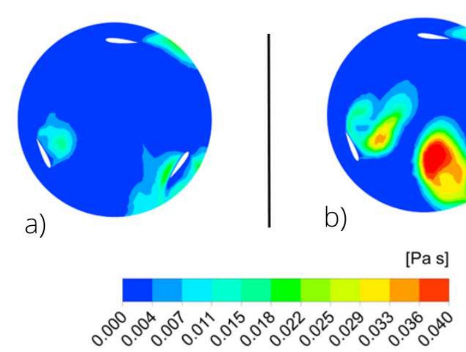

Fig. 9. Turbulent viscosity: (a) twist angle = $15°$; (b) twist angle = $60°$.

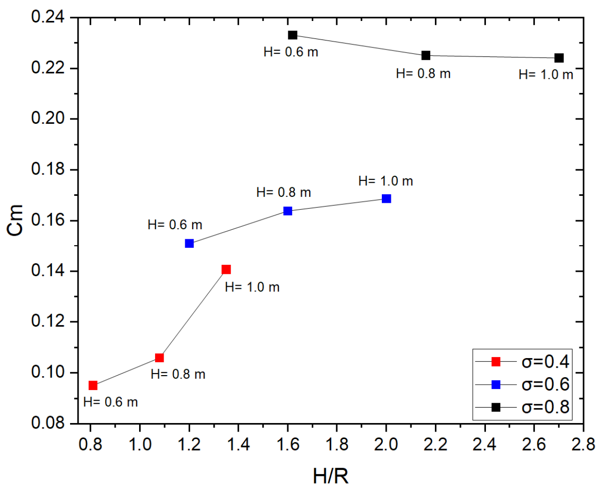

Fig. 10. Variation of torque coefficient with aspect ratio of the turbine with $45°$ twist angle.

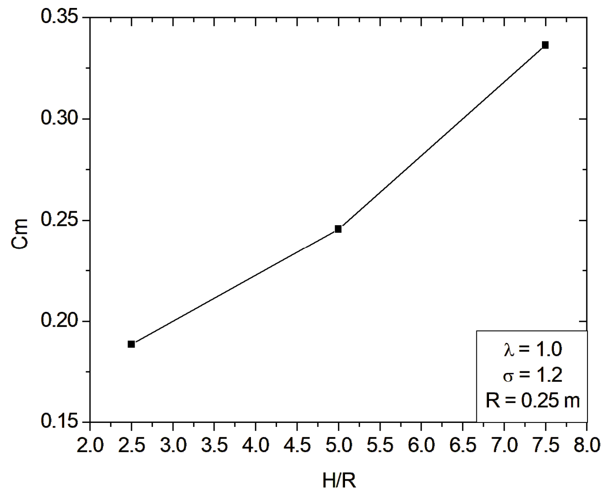

Fig. 11. Relation between high H/R values and torque coefficient for a turbine with $45°$ twist angle.

Unlike the previous study, where the solidity varied, in Fig. 11 the solidity remained constant, $\sigma = 1.2$ and there is a reduction in the incident wind speed to 6 m/s as previously stated. Thus, high aspect ratio values, precisely 2.5, 5.0 and 7.5, are obtained. The value of $H/R = 7.5$ is shown by Kirke [45], showing that to obtain maximum power, values higher than this should be preferred.

The increase in the H/R ratio led to an increase in the torque coefficient, considering the constant radius and the same σ. The height of the blade is directly related to the increase in the area swept by the turbine. Therefore, it is an expected increase. It is also worth considering that the greater the height of the turbine, the lesser the effect of the blade tip vortices, generating induced drag. The value of λ used in this study is $\lambda = 1$, therefore the value of the power coefficient follows the torque coefficient, having the same value.

4. Conclusions

The present numerical study investigated differences between Darrieus vertical axis wind turbine with straight blades and twisted blades. The main operational principle of the device was well reproduced by the present computational model, which was verified by a straight blades' configuration.

Therefore, the performance of the turbine was investigated through the analysis of the turbine torque coefficient, being possible to analyze the influence of the twist angle.

With the results obtained in this study it was observed that as the turbine torsion angle increased, the resulting torque coefficient decreased. This effect was mainly due to the reduction of the lift force caused by the reduction of pressure drop between the two sides of the twisted blades, as well as the perturbation of turbulent flow in the region among the blades. These results were evidenced in the pressure and turbulent viscosity fields. On the other hand, the torque fluctuations were reduced, smoothing the turbine movement. The latter behavior agreed with the previous findings of literature, as pointed in Tjiu et al. [19]. The twisted blade reduced the torque fluctuations up to 55%, which is beneficial for the operation of the turbine. However, the magnitude of C_m also decreased with the twisted angle, which did not agree with the behavior mentioned in Ref. [19] and showing the importance to study various design parameters of twisted-blades turbines.

Even with a decrease in the average torque coefficient, the $35°$ twist angle obtained a good balance between smoothing the torque fluctuation and the magnitude of the average torque coefficient, proving to be a good choice of value to be adopted for the angle, considering that within the angles studied, it was the one that presented the highest level in the torque coefficient.

Another analysis carried out was the influence of solidity on the twisted blade turbine. It was found that an increase in σ generates an increase in the torque coefficient, which reached 59% in the study carried out. In this study, the same σ values found in [14] were used, changing the turbine radius and the chord of the aerodynamic profile, similarly to the previous investigations for straight blade turbines. Results indicated that σ was one of the main factors that influenced both the torque coefficient and the power coefficient. The increase in solidity also increased the peak power that the turbine can reach.

Another parameter analyzed was the aspect ratio, varying the height of the turbine. It was observed that increasing the aspect ratio for low σ values directly influenced the torque coefficient, which reached to an increase of 34%. This relationship was shown to be smaller when σ is greater, but with an opposite behavior, where there was a drop in the torque coefficient with the increase in the aspect ratio, for the applied model. When analyzing high aspect ratio values (above 2.5), the increase in aspect ratio resulted in an increase in the torque coefficient, mainly due to the large increase in the height of the turbine, which in turn increased the area swept by the turbine blades. It is worth mentioning that the increase in the height of the turbine is directly related to the cost of producing it. For constant λ and σ, differences of nearly 80% on C_m were found when $H/R = 2.5$ and 7.5 were compared.

The authors also recommend, as proposal for future studies, the investigation of the problem under other conditions as for other aspect ratios (H/R), blades profiles and dimensions and other flow conditions as intensity of the wind.

Author Contributions

R.S. Vieira planned the scheme, validation, software, formal analysis, and investigation; A. Pavlovic performed the investigation, found resource, data curation and prepared visualization; C. Fragassa planned the methodology, formal analysis, data curation, found resource. E.D. dos Santos planned the scheme, formal analysis, found resource, supervision, administration, and funding acquisition. A.P. Petry planned the scheme, methodology, formal analysis, supervision, project administration, funding acquisition. The manuscript was written through the contribution of all authors. All authors discussed the results, reviewed, and approved the final version of the manuscript.

Acknowledgments

The authors E.D. dos Santos and A.P. Petry thank CNPq for research grant (Processes: 308396/2021-9 and 317432/2021-4). The authors also thank CNPq for financial support in Call CNPq/MCTI N° 10/2023 - Universal (Process: 403408/2023-7).

Conflict of Interest

The authors declared no potential conflicts of interest concerning the research, authorship, and publication of this article.

Funding

This research received no external funding.

Data Availability Statements

The data presented in this study are available on request from the corresponding author. The data are not publicly available due to privacy reasons.

References

[1] Share of electricity production from wind. Our World in Data. Retrieved 15 August 2023. https://ourworldindata.org/grapher/share-electricity-wind
[2] Wiser, R., Bolinger, M., *Wind Technologies Market Report*, U.S. Department of Energy, 2017.
[3] McKenna, R., Pfenninger, S., Heinrichs, H., Schmidt, J., Staffell, I., Bauer, C., Gruber, K., Hahmann, A.N., Jansen, M., Klinger, M., Landwehr, N., Larsén, X.G., Lilliestam, J., Pickering, B., Robinius, M., Tröndle, T., Turkovska, O., Wehrle, S., Weinand, J.M., Wohland, J., High-resolution large-scale onshore wind energy assessments: a review of potential definitions, methodologies and future research needs, *Renewable Energy*, 182, 2022, 659-684.
[4] Dupré la Tour, M.-A., Photovoltaic and wind energy potential in Europe – A systematic review, *Renewable and Sustainable Energy Reviews*, 179, 2023, 113189.
[5] Pope, K., Dincer, I., Naterer, G.F., Energy and exergy efficiency comparison of horizontal and vertical axis wind turbines, *Renewable Energy*, 35(9), 2010, 2102-2113.
[6] Stathopoulos, T., Alrawashdeh, H., Al-Quraan, A., Blocken, B., Dilimulati, A., Paraschivoiu, M., Pilay, P., Urban wind energy: Some views on potential and challenges, *Journal of Wind Engineering and Industrial Aerodynamics*, 179, 2018, 146-157.
[7] Kumar, P.M., Sivalingam, K., Narasimalu, S., Lim, T.-C., Ramakrishna, S., Wei, H., A Review on the Evolution of Darrieus Vertical Axis Wind Turbine: Small Wind Turbines, *Journal of Power and Energy Engineering*, 7, 2019, 27-44.
[8] Ferroudji, F., Khelifi, C., Structural Strength Analysis and Fabrication of a Straight Blade of an H-Darrieus Wind Turbine, *Journal of Applied and Computational Mechanics*, 7, 2021, 1276-1282.
[9] Marzec, Ł., Bulinski, Z., Krysinski, T., Tumidajski, J., Structural optimisation of H-Rotor wind turbine blade based on one-way Fluid Structure Interaction approach, *Renewable Energy*, 216, 2023, 118957.
[10] Karimian, S.M.H., Abolfazl, A., Performance investigation of a new Darrieus vertical axis wind turbine, *Energy*, 91, 2020, 116551.
[11] Pongduang, S., Kayankannavee, C., Tiaple, Y., Experimental investigation of helical tidal turbine characteristics with different twists, *Energy*, 79, 2015, 409–414.
[12] Niblick, A., *Experimental and analytical study of helical crossflow turbines for a tidal micropower generation system*, Master Thesis, Seattle, WA, University of Washington, 2012.
[13] Sagharichi, A., Zamani, M., Ghasemi, A., Effect of solidity on the performance of variable-pitch vertical axis wind turbine, *Energy*, 161, 2018, 753-775.
[14] Lee, Y., Lim, H., Numerical study of the aerodynamic performance of a 500W Darrieus-type vertical-axis wind turbine, *Renewable Energy*, 83, 2015, 407-415.
[15] Marsh, P., Ranmuthugala, D., Penesis, I., Thomas, G., Numerical investigation of the influence of blade helicity on the performance characteristics of vertical axis tidal turbines, *Renewable Energy*, 81, 2015, 926-935.
[16] Elkhoury, M., Kiwata, T., Aoun, E., Experimental and numerical investigation of a three-dimensional vertical-axis wind turbine with variable pitch, *Journal of Wind Engineering and Industrial Aerodynamics*, 139, 2015, 111–123.
[17] Satrio, D., Utama, I.K.A.P., Experimental investigation into the improvement of self-starting capability of vertical-axis tidal current turbine, *Energy Reports*, 7, 2021, 4587–4594.
[18] Le, T.Q., Lee, K., Park, J., Ko, J.H., Flow-driven rotor simulation of vertical axis tidal turbines: A comparison of helical and straight blades, *International Journal of Naval Architecture and Ocean Engineering*, 6, 2014, 257-268.
[19] Tjiu, W., Marnoto, T., Mat, S., Ruslan, M.H., Sopian, K., Darrieus vertical axis wind turbine for power generation I: Assessment of Darrieus VAWT configurations, *Renewable Energy*, 75, 2015, 50-67.
[20] Kavade, R., Ghanegaonkar, P., Performance Analysis of Small-Scale Variable Pitch Vertical Axis Wind Turbine, *FME Transactions*, 50, 2022, 322-330.
[21] Abdelsalam, A.M., Kotb, M.A., Khaled Yousef, K., Sakr, I.M., Performance study on a modified hybrid wind turbine with twisted Savonius blades,

Energy Conversion and Management, 241, 2021, 114317.
[22] Kumar, R., Sarkar, S., Effect of design parameters on the performance of helical Darrieus hydrokinetic turbines, *Renewable and Sustainable Energy Reviews*, 162, 2022, 112431.
[23] Wu, X., Wu, H., Zuo, L., Chen, B., The effect of the blade number on a crossflow hydrokinetic turbine, *IFAC-PapersOnLine*, 55, 2022, 62-67.
[24] Al-dabbagh, M.A., Yuce, M.I., Simulation and comparison of helical and straight bladed hydrokinetic turbines, *International Journal of Renewable Energy Research*, 8, 2018, 504-513.
[25] Mohamed, O.S., Elbaz, A.M.R., Bianchini, A., A better insight on physics involved in the self-starting of a straight-blade Darrieus wind turbine by means of two-dimensional Computational Fluid Dynamics, *Journal of Wind Engineering & Industrial Aerodynamics*, 218, 2021, 1-3.
[26] Dezvareh, R., Evaluation of Turbulence on the Dynamics of Monopile Offshore Wind Turbine under the Wave and Wind Excitations, *Journal of Applied and Computational Mechanics*, 5, 2019, 704-716.
[27] Fertahi, S., Samaouali, A., Kadiri, I., CFD comparison of 2D and 3D aerodynamics in H-Darrieus prototype wake, *e-Prime - Advances in Electrical Engineering, Electronics and Energy*, 4, 2023, 100178.
[28] Kaya, A.F., Tanürün, H.E., Acır A., Numerical investigation of radius dependent solidity effect on H-type vertical axis wind turbines, *Politeknik Dergisi*, 25, 2022, 1007-1019.
[29] Qamar, S.B., Janajreh, I., A comprehensive analysis of solidity for cambered darrieus VAWTs, *International Journal of Hydrogen Energy*, 42, 2014, 19420-19431.
[30] Abdolahifar, A., Karimian, S.M.H., A comprehensive three-dimensional study on Darrieus vertical axis wind turbine with slotted blade to reduce flow separation, *Energy*, 248, 2022, 123632.
[31] Potsis, T., Tominaga, Y., Stathopoulos, T., Computational wind engineering: 30 years of research progress in building structures and environment, *Journal of Wind Engineering and Industrial Aerodynamics*, 234, 2023, 105346.
[32] Tominaga, Y., Wang, L., Zhai, Z., Stathopoulos, T., Accuracy of CFD simulations in urban aerodynamics and microclimate: Progress and challenges, *Building and Environment*, 243, 2023, 110723.
[33] Kasmaiee, S., Tadjfar, M., Kasmaiee, S., Optimization of Blowing Jet Performance on Wind Turbine Airfoil Under Dynamic Stall Conditions Using Active Machine Learning and Computational Intelligence, *Arabian Journal for Science and Engineering*, 49, 2024, 1771–1795.
[34] Kasmaiee, S., Tadjfar, M., Kasmaiee, S., Machine learning-based optimization of a pitching airfoil performance in dynamic stall conditions using a suction controller, *Physics of Fluids*, 35, 2023, 095121.
[35] Wilcox, D.C., *Turbulence Modelling for CFD*, DCW Industries, La Canada, USA, 2002.
[36] Launder, B.E., Spalding, D.B., *Mathematical Models of Turbulence*, Academic Press, London, 1972.
[37] Hinze, J.O., *Turbulence*, McGraw-Hill, New York, USA, 1975.
[38] Menter, F.R., Kuntz, M., Langtry, R., Ten years of industrial experience with the SST turbulence model, *In: Turbulence, Heat and Mass Transfer*, Hanjalic, K., Nagano, Y. and Tummers, M., Eds., Begell House: Danbury, CT, USA, 2003.
[39] Ansys, Ansys® Fluent User's Guide, version 2021 R2, 2021.
[40] Patankar, S., *Numerical Heat Transfer and Fluid Flow*, CRC Press, Boca Raton, USA, 1980.
[41] Versteeg, H.K., Malalasekera, W., *An introduction to computational fluid dynamics: the finite volume method*, Pearson/Prentice Hall, Harlow, UK, 2007.
[42] Balduzzi, F., Bianchini, A., Ferrara, G., Ferrari, L., Dimensionless numbers for the assessment of mesh and time-step requirements in CFD simulations of Darrieus wind turbines, *Energy*, 97, 2016, 246-261.
[43] Schlichting, H., Gersten, K., *Boundary-Layer Theory*, 8 ed., Springer, Berlin, Germany, 2003.
[44] Freire, A.P., Menut, P.P., Su, J., *Turbulência*, Volume 1., Rio de Janeiro, Brasil, ABCM – Associação Brasileira de Ciências Mecânicas, 2002.
[45] Kirke, B.K., *Evaluation of self-starting vertical axis wind turbines for stand-alone applications*, PhD Thesis, School of Engineering, Griffith University, Australia, 1998.

ORCID iD

Rodrigo S. Vieira https://orcid.org/0000-0002-3382-9638
Ana Pavlovic https://orcid.org/0000-0003-2158-1820
Cristiano Fragassa https://orcid.org/0000-0003-0046-8810
Elizaldo Domingues dos Santos https://orcid.org/0000-0003-4566-2350
Adriane P. Petry https://orcid.org/0000-0002-1272-5303

How to cite this article: Vieira R.S., Pavlovic A., Fragassa C., dos Santos E.D., Petry A.P. Complexity-Aware Design Analysis of the Efficiency in Darrieus Vertical Axis Wind Turbines, *J. Appl. Comput. Mech.*, 11(1), 2025, 264-273. https://doi.org/10.22055/jacm.2024.46304.4496